

RESEARCH ARTICLE



## Promising anti-*Helicobacter pylori* and anti-inflammatory metabolites from unused parts of *Phoenix dactylifera* CV 'Zaghloul': *in vitro* and *in silico* study

Nada Elhefni<sup>a</sup>, Sherif S. Ebada<sup>b</sup>, Marwa M. Abdel-Aziz<sup>c</sup>, El-Sayed M. Marwan<sup>a</sup>, Saleh El-Sharkawy<sup>a</sup> and Mona El-Neketi<sup>a</sup>

<sup>a</sup>Department of Pharmacognosy, Faculty of Pharmacy, Mansoura University, Mansoura, Egypt; <sup>b</sup>Department of Pharmacognosy, Faculty of Pharmacy, Ain-Shams University, Cairo, Egypt; <sup>c</sup>The Regional Center for Mycology and Biotechnology, Al-Azhar University, Cairo, Egypt

### ABSTRACT

**Context:** Date palm waste is an agricultural waste that accumulates in massive amounts causing serious pollution and environmental problems.

**Objectives:** Date palm trees, *Phoenix dactylifera* Linn CV 'Zaghloul' (Arecaceae) grown in Egypt, leave behind waste products that were investigated to produce compounds with anti-*Helicobacter pylori* and anti-inflammatory activities.

**Materials and methods:** Chromatographic workup of *P. dactylifera* aqueous methanol extract derived from fibrous mesh and fruit bunch (without fruit) afforded a new sesquiterpene lactone derivative, phodactolide A (**1**), along with ten known compounds (**2–11**), primarily identified as polyphenols. Chemical structures were unambiguously elucidated based on mass and 1D/2D NMR spectroscopy. All isolated compounds were assessed for their activities against *H. pylori* using broth micro-well dilution method and clarithromycin as a positive control. The anti-inflammatory response of isolated compounds was evaluated by inhibiting cyclooxygenase-2 enzyme using TMPD Assay followed by an *in silico* study to validate their mechanism of action using celecoxib as a standard drug.

**Results:** Compounds **4**, **6** and **8–10** exhibited potent anti-*H. pylori* activity with MIC values ranging from 0.48 to 1.95 µg/mL that were comparable to or more potent than clarithromycin. For COX-2 inhibitory assay, **4**, **7** and **8** revealed promising activities with IC<sub>50</sub> values of 1.04, 0.65 and 0.45 µg/mL, respectively. These results were verified by molecular docking studies, where **4**, **7** and **8** showed the best interactions with key amino acid residues of COX-2 active site.

**Conclusion:** The present study characterizes a new sesquiterpene lactone and recommends **4** and **8** for future *in vivo* studies as plausible anti-ulcer remedies.

### ARTICLE HISTORY

Received 18 November 2022  
Revised 5 March 2023  
Accepted 4 April 2023

### KEYWORDS

Date palm waste; COX-2 inhibitors; molecular docking

### Introduction

A tremendous amount of agro-industrial waste is being produced worldwide annually. This is due to the enormous expansion of agroindustrial practices as well as human civilization (Faiad et al. 2022). The number of date palm trees exceeds 120 million throughout the world producing annually several million tons of dates (Aydeniz-Güneşer 2022). In Egypt, agricultural wastes are accumulating in large quantities causing environmental drawbacks including serious health hazards. Partial resolution of this problem can be achieved by utilizing this waste economically to produce valuable chemicals and pharmaceuticals (Rao and Rathod 2019). Egypt is one of the largest date palm producers (1.47 million tons in 2012; MT/Y) which also produce a large amounts of agricultural waste. Date palm waste, in the Middle East and North Africa (MENA) region, constitute about 2.8 MT/Y in the form of fruitless bunch, fibrous mesh, fronds and seeds. Thus, agro-industrial waste of date palm represent a serious disposal problem (Jonoobi et al. 2019; Aydeniz-Güneşer 2022; Faiad et al. 2022).

*Phoenix dactylifera* Linn (palm tree) is a member of Arecaceae family, which comprises approximately 235 genera including 4000 species, and it is one of the most cultivated palms among the fourteen *Phoenix* species (Aydeniz-Güneşer 2022). Date palm is a rich source for fatty materials, carotenoids, polyphenols (such as phenolic acids, flavonoids, isoflavones and lignans), tannins and sterols (Bentrad and Hamida-Ferhat 2020; Suleiman et al. 2021).

Although date palm is primarily used for nutrition, many varieties of *P. dactylifera* have antimicrobial, antifungal, anti-inflammatory, anticancer, immunostimulant and hemolytic properties (Baliga et al. 2011), along with its activities as antioxidant, for improving male and female fertility, hepatoprotective, nephroprotective and for tumor growth inhibition (El-Far et al. 2019). Therefore, our research interest was directed toward date palm agricultural waste as a probable source of bioactive metabolites that can be later developed into phytopharmaceuticals.

The primary etiological agent of stomach cancer, peptic ulcers and/or chronic gastritis is thought to be *Helicobacter pylori*, which is prevalent worldwide (Abou Baker 2020). Several

**CONTACT** Mona El-Neketi  [melneketi@mans.edu.eg](mailto:melneketi@mans.edu.eg)  Department of Pharmacognosy, Faculty of Pharmacy, Mansoura University, 35516 Mansoura, Egypt

 Supplemental data for this article can be accessed online at <https://doi.org/10.1080/13880209.2023.2200841>.

© 2023 The Author(s). Published by Informa UK Limited, trading as Taylor & Francis Group.

This is an Open Access article distributed under the terms of the Creative Commons Attribution-NonCommercial License (<http://creativecommons.org/licenses/by-nc/4.0/>), which permits unrestricted non-commercial use, distribution, and reproduction in any medium, provided the original work is properly cited. The terms on which this article has been published allow the posting of the Accepted Manuscript in a repository by the author(s) or with their consent.

therapeutic protocols for *H. pylori* eradication have been implemented over the last four decades. The most common is clarithromycin-based triple therapy, which is a proton-pump inhibitor (PPI) combined with amoxicillin and clarithromycin (Galal et al. 2021).

Several natural products possess anti-*H. pylori* activities. Such potential mechanisms include urease inhibition, DNA damage, protein synthesis inhibition and anti-inflammatory effects along with the anti-*H. pylori* effects by inhibiting bacterial enzymes such as dihydrofolate reductase and myeloperoxidase *N*-acetyltransferase (Wang 2014; Abou Baker 2020).

Inflammation is a complex biological response to a harmful stimulus that can range from a localized to a generalized response and is mediated by prostaglandins (PGs) that are major metabolites of cyclooxygenase (COX) enzyme, which exist in different isoforms, COX-1 and COX-2 (Bonacorsi et al. 2009). Cyclooxygenase-2 (COX-2) is involved in the induction of gastric cancer in *H. pylori* infected patients (Wong et al. 2012). *H. pylori* can trigger COX-2 overexpression. Thus, the intervention with a COX-2 inhibitor will prevent or stop *H. pylori*-related carcinogenesis process (Wong et al. 2012). Therefore, the present study is directed toward the search for new and effective *H. pylori* and COX-2 inhibitors that might lead to the development of new peptic ulcer therapeutics.

*In silico* molecular docking is an effective technique of drug design that predicts the ligand's optimal orientation with respect to a potential therapeutic target. This method uses both time and labor-efficiency (Roy et al. 2019). Following the conduction of biological assays, a molecular docking study was performed using isolated compounds in order to ascertain their binding to the COX-2 enzyme active site and provide an explanation for their bioactivity(ies), if any.

This study describes isolation and characterization of a new sesquiterpene lactone along with ten known compounds from date palm waste illustrating their potential activities and possible roles for developing valuable phytopharmaceuticals.

## Materials and methods

### Plant materials

Waste parts (fibrous mesh and fruitless bunch) of *P. dactylifera* L. (CV 'Zaghloul') were collected from around the University of Mansoura campus, Egypt in February 2019. The plant was identified by Prof. Dr. Ibrahim Mashaly, Ecology and Botany Department, Faculty of Sciences, Mansoura University. A specimen (voucher no. NSM595926) was kept at Department of Pharmacognosy, Faculty of Pharmacy, Mansoura University. The plant materials were shade-dried, milled to particle size 1.25 µm mesh size and kept for further investigation.

### General experimental procedures

Nuclear Magnetic Resonance spectra ( $^1\text{H}$ ,  $^{13}\text{C}$ , APT, DEPT135,  $^1\text{H}$ - $^1\text{H}$  COSY, HMBC, HSQC and ROESY) were recorded on Bruker DRX 400 NMR spectrometer (Bruker Daltonics Inc., MU, Egypt). Deuterated NMR solvents including chloroform-*d*, methanol-*d*<sub>4</sub> and DMSO-*d*<sub>6</sub> were used. Chemical shifts were measured in parts per million (ppm) using TMS as an internal standard. HRESIMS was determined using LCMS-IT-TOF (Shimadzu, Tokyo, Japan). Column chromatography was performed using silica gel G 60 M (Merck, Germany) or Sephadex LH20 (Pharmacia, USA) as stationary phases. Thin-layer

chromatography (TLC) plates pre-coated with silica gel 60 GF<sub>254</sub> (20 × 20 cm × 0.2 mm thick, Merck) were used and spots were made visible by spraying vanillin-sulfuric acid reagent.

### Extraction and fractionation

#### Extraction and isolation of compounds from the fibrous mesh

The air-dried powdered fibrous mesh of *P. dactylifera* (5 kg) was extracted by maceration using (8 × 4 L) 50% hydro-methanol solution (50:50, v/v MeOH: H<sub>2</sub>O). The solvent was evaporated under reduced pressure and the extract was dried over anhydrous CaCl<sub>2</sub> in a desiccator. The obtained extract (205 g) was dissolved in 100 mL 50% aq. MeOH, and successively extracted with petroleum ether (3 × 0.5 L), methylene chloride (6 × 1 L), ethyl acetate (6 × 1 L) and finally water-saturated *n*-butanol (3 × 1 L). The solvent, in each case, was evaporated to dryness under reduced pressure to give pet. ether fraction (2.0 g), methylene chloride fraction (8.0 g), ethyl acetate fraction (6.5 g) and *n*-butanol fraction (22.0 g), respectively.

The obtained crude pet. ether fraction (2.0 g) was purified using multiple steps of silica gel column chromatography (CC: 60 × 3 cm) in a gradient elution with pet. ether/CH<sub>2</sub>Cl<sub>2</sub> and CH<sub>2</sub>Cl<sub>2</sub>/EtOAc in different ratios of increasing polarity. Based on TLC, similar fractions were combined. Two subfractions were selected for further purifications using silica gel CC and a gradient elution of previously mentioned solvent systems. Subfraction (45–52; 1.2 g) afforded **2** (4.2 mg), while subfraction (69–81; 700 mg) afforded **3** (80 mg) and **1** (3.4 mg).

The CH<sub>2</sub>Cl<sub>2</sub> fraction (8.0 g) was chromatographed over silica gel column (100 × 3 cm), using a gradient elution of pet. ether/EtOAc and EtOAc/MeOH where similar fractions were combined. Subfraction (24–46; 180 mg) was further fractionated on silica gel column (32 × 1.5 cm) using pet. ether/EtOAc in a gradient elution which furnished **9** (11.0 mg), while subfraction (83–109; 120 mg) yielded **6** (14.0 mg) by precipitation.

The EtOAc fraction (6.5 g) was subjected to silica gel column (65 × 3 cm) eluted with CH<sub>2</sub>Cl<sub>2</sub>/MeOH mixtures of increasing polarity. Subfraction (28–33; 40 mg), was selected and purified over Sephadex LH20 column, eluted with methanol (100%) to afford **10** (2.0 mg), while subfractions (34–43) provided **7** (3.2 mg) as precipitate and purified through crystallization. The *n*-butanol fraction (22.0 g) was applied to a silica gel column (75 × 4 cm) using a gradient elution of EtOAc/MeOH, to afford one promising group of similar subfractions. Compound **11** (33.0 mg) was obtained from sub-fractions (22–31; 150 mg) by crystallization using CH<sub>2</sub>Cl<sub>2</sub>/MeOH (1:1 v/v).

#### Extraction and isolation of compounds from the fruitless bunch

About 10 kg of powdered air-dried fruitless bunch was similarly treated using 50% hydro-methanol solution to yield a crude extract (1 kg). Solvent fractionation yielding pet. ether fraction (96.0 g), CH<sub>2</sub>Cl<sub>2</sub> fraction (56.0 g), EtOAc fraction (35.0 g) and *n*-butanol (60.0 g). CH<sub>2</sub>Cl<sub>2</sub> fraction (56.0 g) and EtOAc fraction (35.0 g) were separately subjected to vacuum liquid chromatography (VLC), using silica gel stationary phase. A gradient elution with: 100% *n*-hexane, *n*-hexane/EtOAc, EtOAc, CH<sub>2</sub>Cl<sub>2</sub>, CH<sub>2</sub>Cl<sub>2</sub>/MeOH, and finally with 100% MeOH was used. Similar fractions were combined based on TLC monitoring. Methylene chloride subfraction (eluted from VLC with *n*-hexane/EtOAc, 50:50 v/v) was further fractionated over silica gel column implementing gradient elution scheme using CH<sub>2</sub>Cl<sub>2</sub>/EtOAc.

The obtained subfractions (20–21), yielded **5** (9.5 mg) by precipitation, while the subfractions (23–24), was further purified over Sephadex LH20 column using MeOH (100%) as a mobile phase to afford **4** (8.0 mg). Similarly, EtOAc subfractions eluted from VLC with *n*-hexane/EtOAc (40:60–5:95 v/v) were combined and purified on normal phase silica gel CC using gradient elution of CH<sub>2</sub>Cl<sub>2</sub>/EtOAc. Subfraction (26–32) was selected and chromatographed over Sephadex LH20 column using MeOH (100%) to give **10** (4.0 mg), while the grouped EtOAc subfraction eluted from VLC with CH<sub>2</sub>Cl<sub>2</sub>/MeOH (90:10–80:20 v/v) was separated on a silica gel column with a gradient of CH<sub>2</sub>Cl<sub>2</sub>/MeOH as eluent, to yield subfraction (64–72) from which **8** (10.0 mg) was precipitated.

### In vitro assay against *Helicobacter pylori*

All isolated compounds were evaluated for their antibacterial activity against *H. pylori*, using a micro-well dilution method (Bonacorsi et al. 2009). Suspensions of *H. pylori* inoculum were prepared at 10<sup>6</sup> CFU/mL. The samples and positive control (clarithromycin) were dissolved in dimethyl sulfoxide (DMSO) and applied to a 96-well plate at concentrations of 125–0.24 μg.

Dose-response curves were used to calculate the sample concentration required to provide 90% inhibition (MIC 90). Using an automatic ELISA microplate reader at 620 nm, the MIC was recorded at the lowest concentration at which there was no change in the MTT color. The MIC values were measured three times (Bonacorsi et al. 2009; Galal et al. 2021).

### Evaluation of in vitro anti-inflammatory activity against cyclooxygenase-2 enzyme (COX-2)

All isolated compounds were prepared at 125 to 0.98 μg/mL serial dilutions to assess their anti-inflammatory potential against the COX-2 enzyme. The results of oxidation reaction of *N,N,N,N*-tetramethyl-*p*-phenylenediamine (TMPD) with arachidonic acid were used for the COX (EC1.14.99.1) activity evaluation. This assay was performed as previously reported in the literature with slight modifications (Petrovic and Murray 2010; Amessis-Ouchemoukh et al. 2014). The enzyme activity inhibition was monitored by the increase in absorbance at 611 nm using a microplate reader (BIOTEK; USA). The percentage of inhibition was calculated using the equation: Inhibitory activity (%) = (1 - A<sub>s</sub>/A<sub>c</sub>) × 100, where A<sub>s</sub> is the absorbance of test compound and A<sub>c</sub> is the absorbance of control. The efficacy of the isolates and celecoxib (reference compound) to inhibit COX-2 isoenzyme were measured in terms of IC<sub>50</sub> (the concentration causing 50% enzyme inhibition).

### Molecular simulation studies

The molecular simulation studies including docking simulation and three dimensional-surface mapping were used to predict the binding interactions between the tested compounds (**1–11**) and the cyclooxygenase-2 enzyme (COX-2) active site amino acids residues and comparing their results to celecoxib (reference COX-2 inhibitor).

### Ligand and protein preparation

Isolated compound structures, in their neutral forms, were prepared in their most stable conformers for docking into the COX-

2 active site. Energy minimization was done using the MMFF94 technique with root mean square (RMS) gradient of 0.01 kcal/mol Å. The tested compounds (**1–11**) were docked into the active site of human cyclooxygenase-2 (COX-2) (ID: 5IKQ) (Orlando and Malkowski 2016). Targets were prepared for docking by adding the hydrogen atoms, followed by automatic structure corrections and target potential fixation. The active site was determined as the region of target enzyme within 10 Å from the ligand (Qandeel et al. 2020).

## Results

### Characterization of isolated compounds

About 205 g of hydro-methanolic (50%) extract obtained from extraction of 5 kg of *P. dactylifera* fibrous mesh. The extract was subjected to organic solvents fractionation and purification to give compounds **1–3**, **6**, **7** and **9–11** in substantial amounts. The fruitless bunch produced compounds **4**, **5**, **8** and **10**. All isolated compounds were purified using different chromatographic procedures and were subjected to MS, 1D and 2D NMR spectroscopic analyses. Chemical identities of isolated compounds were unambiguously determined based on spectroscopic analyses and on the comparison with the reported data.

A new sesquiterpene lactone derivative (**1**) was isolated from date palm tree waste along with ten known compounds (Figure 1), namely, pimaric acid (**2**) (Dang et al. 2005), vaginatin (**3**) (Yang et al. 2008), syringaresinol (**4**) (Malee 2011), chrysoeriol (**5**) (Bashyal et al. 2019), apigenin (**6**) (Alwahsh et al. 2015), luteolin (**7**) (Park et al. 2011), diosmetin-7-*O*-β-D-glucopyranoside (**8**) (Lee et al. 2012), methylparaben (**9**) (Yoshioka et al. 2004), *p*-hydroxybenzoic acid (**10**) (Yoshioka et al. 2004) and methyl β-D-xylopyranoside (**11**) (McEwan et al. 1982).

### Structure elucidation of compound 1

Compound **1** was isolated from the petroleum ether fraction of the fibrous mesh as a colorless amorphous powder. Its molecular formula was determined to be C<sub>23</sub>H<sub>30</sub>O<sub>7</sub> based on HRESIMS that exhibited a pseudomolecular ion peak at *m/z* 419.2063 [M + H]<sup>+</sup> (calcd for C<sub>23</sub>H<sub>31</sub>O<sub>7</sub>, 419.2070) indicating nine degrees

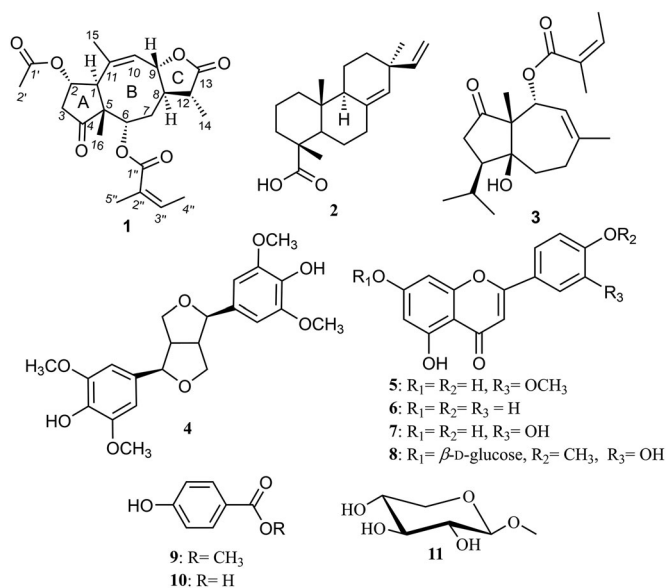
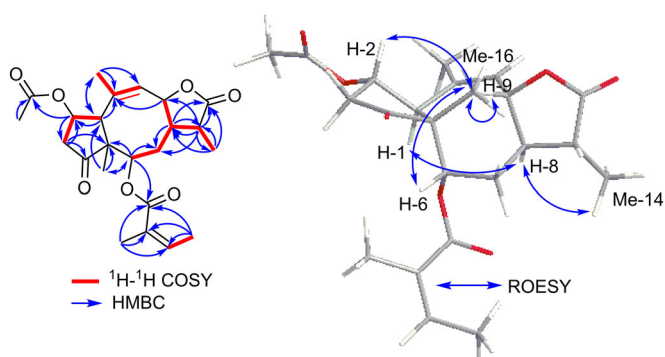


Figure 1. Chemical structures of **1–11**.

**Table 1.**  $^1\text{H}$  NMR (400 MHz) and  $^{13}\text{C}$  NMR (100 MHz) data of **1** in chloroform-*d*.

| Position | $\delta_{\text{C}}$   | $\delta_{\text{H}}$ ( <i>J</i> in Hz) |
|----------|-----------------------|---------------------------------------|
| 1        | 41.3, CH              | 2.94 m                                |
| 2        | 71.5, CH              | 4.79 m                                |
| 3        | 29.5, CH <sub>2</sub> | Ha: 2.27 m<br>Hb: 2.07 m              |
| 4        | 218.0, C              |                                       |
| 5        | 39.1, C               |                                       |
| 6        | 76.2, CH              | 5.00 dd ( <i>J</i> = 11.4, 6.2)       |
| 7        | 26.2, CH <sub>2</sub> | Ha: 1.83 m<br>Hb: 1.65 m              |
| 8        | 36.1, CH              | 2.68 m                                |
| 9        | 78.5, CH              | 4.59 dd ( <i>J</i> = 9.4, 6.2)        |
| 10       | 119.4, CH             | 5.32 br s                             |
| 11       | 133.6, C              |                                       |
| 12       | 37.6, CH              | 2.93 m                                |
| 13       | 178.7, C              |                                       |
| 14       | 10.4, CH <sub>3</sub> | 1.20 d ( <i>J</i> = 7.2)              |
| 15       | 22.0, CH <sub>3</sub> | 1.88 m                                |
| 16       | 22.2, CH <sub>3</sub> | 1.07 s                                |
| 1'       | 170.2, C              |                                       |
| 2'       | 21.7, CH <sub>3</sub> | 1.96 s                                |
| 1''      | 168.4, C              |                                       |
| 2''      | 128.0, C              |                                       |
| 3''      | 137.7, CH             | 6.02 qd ( <i>J</i> = 7.2, 1.5)        |
| 4''      | 15.9, CH <sub>3</sub> | 1.93 dd ( <i>J</i> = 7.2, 1.5)        |
| 5''      | 20.6, CH <sub>3</sub> | 1.83 t ( <i>J</i> = 1.5)              |

of unsaturation. The  $^{13}\text{C}$  NMR and HMQC spectra indicated the presence of 23 different carbon peaks that can be distinguished into four carbonyl carbons ( $\delta_{\text{C}}$  218.0, 178.7, 170.2, 168.4), four olefinic carbons ( $\delta_{\text{C}}$  137.7, 133.6, 128.0, 119.4), one quaternary aliphatic carbon ( $\delta_{\text{C}}$  39.1), three oxygenated tertiary carbons ( $\delta_{\text{C}}$  78.5, 76.2, 71.5), three methine carbons ( $\delta_{\text{C}}$  41.3, 37.6, 36.1), two methylene carbons ( $\delta_{\text{C}}$  29.5, 26.2) and six methyl carbons ( $\delta_{\text{C}}$  22.2, 22.0, 21.7, 20.6, 15.9, 10.4). The existence of four carbonyl carbons and four olefinic carbons gives clue for six of the nine degrees of unsaturation deduced from its molecular formula. Hence, compound **1** was expected to comprise a tricyclic moiety.  $^1\text{H}$  NMR and HSQC spectral data (Table 1) displayed resonances and key correlations of an angeloyl moiety, namely,  $\delta_{\text{H}}$  6.02 (1H, qd, *J* = 7.2, 1.5 Hz),  $\delta_{\text{H}}$  1.93 (3H, dd, *J* = 7.20, 1.5 Hz) and  $\delta_{\text{H}}$  1.83 (3H, t, *J* = 1.5 Hz) that were directly correlated to  $\delta_{\text{C}}$  137.7,  $\delta_{\text{C}}$  15.9 and  $\delta_{\text{C}}$  20.6 ppm, respectively (Xue et al. 2021). In addition, both methyl groups of the angeloyl moiety showed similar long-range ( $J^3$ ) correlations in HMBC spectrum to the same three carbon resonances at  $\delta_{\text{C}}$  168.4,  $\delta_{\text{C}}$  128.0 and  $\delta_{\text{C}}$  137.7 ppm ascribed to C-1'', C-2'' and C-3'', respectively. In addition, the presence of an acetyl moiety was proved *via* the singlet methyl resonance at  $\delta_{\text{H}}$  1.96/ $\delta_{\text{C}}$  21.7 ppm that showed a long-range correlation in HMBC spectrum to a carbonyl carbon ( $\delta_{\text{C}}$  170.2, C-1'). The  $^1\text{H}$ - $^1\text{H}$  COSY spectrum revealed the existence of four different spin systems including three short systems along with an extended branched one as illustrated with the bold red lines in Figure 2. By comparing the obtained spectral data of **1** with the reported literature, it was found to be consistent with a tricyclic sesquiterpene lactone derivative featuring a rare 5/8/3 skeleton (Rustaiyan et al. 1989; Tian et al. 2013). This was undoubtedly evidenced by checking HMBC spectrum that revealed clear long-range correlations from a singlet methyl proton resonance at  $\delta_{\text{H}}$  1.07 to three carbon resonances at  $\delta_{\text{C}}$  41.3 (C-1),  $\delta_{\text{C}}$  71.5 (C-2) and  $\delta_{\text{C}}$  76.2 (C-6) ppm to indicate the position of the singlet methyl group to be at C-5 as in pseudoguaianolide-type sesquiterpene lactone derivatives (Wu, Li, et al. 2012; Wu, Su, et al. 2012; Zhang et al. 2018; Xue et al. 2021). The existence of the rare eight-membered ring (B) in the tricyclic structure of **1** was proved by the presence of an additional

**Figure 2.** Key  $^1\text{H}$ - $^1\text{H}$  COSY, HMBC and ROESY correlations of **1**.**Table 2.** MIC of the isolated compounds against *H. pylori*.

| Compound                          | Mean of <i>H. pylori</i> inhibitory %<br>MIC ( $\mu\text{g/ml}$ ) |
|-----------------------------------|---|
| <b>1</b>                          | NA  |
| <b>2</b>                          | 31.25   |
| <b>3</b>                          | NA  |
| <b>4</b>                          | 0.98  |
| <b>5</b>                          | 3.9   |
| <b>6</b>                          | 1.95  |
| <b>7</b>                          | 3.9   |
| <b>8</b>                          | 0.98  |
| <b>9</b>                          | 1.95  |
| <b>10</b>                         | 0.48  |
| <b>11</b>                         | >125  |
| <b>Clarithromycin<sup>a</sup></b> | 1.95  |

MIC: minimum inhibitory concentration; NA: no activity. <sup>a</sup>The standard used Clarithromycin.

**Table 3.** IC<sub>50</sub> values of COX-2 enzyme inhibition by the isolated compounds.

| Compound                     | IC <sub>50</sub> $\pm$ SD ( $\mu\text{g/ml}$ ) |
|------------------------------|--|
| <b>1</b>                     | NA   |
| <b>2</b>                     | 5.6 $\pm$ 0.14                                 |
| <b>3</b>                     | NA   |
| <b>4</b>                     | 1.04 $\pm$ 0.63                                |
| <b>5</b>                     | 6.6 $\pm$ 0.74                                 |
| <b>6</b>                     | 3.2 $\pm$ 1.4                                  |
| <b>7</b>                     | 0.65 $\pm$ 0.33                                |
| <b>8</b>                     | 0.45 $\pm$ 0.85                                |
| <b>9</b>                     | 14.9 $\pm$ 0.63                                |
| <b>10</b>                    | 2.7 $\pm$ 1.3                                  |
| <b>11</b>                    | 5.9 $\pm$ 1.2                                  |
| <b>Celecoxib<sup>a</sup></b> | 0.28 $\pm$ 0.41                                |

IC<sub>50</sub>: the concentration causing 50% enzyme inhibition; NA: no activity. <sup>a</sup>The standard used Celecoxib.

methylene group at  $\delta_{\text{Ha}}$  1.83/ $\delta_{\text{H}}$  1.65 ppm, directly correlated through HSQC spectrum to a methylene carbon at  $\delta_{\text{C}}$  26.2 ppm. This methylene group was positioned at C-7 by  $^1\text{H}$ - $^1\text{H}$  COSY spectrum and located in between the two methine protons at  $\delta_{\text{H}}$  5.00/ $\delta_{\text{C}}$  76.2 and  $\delta_{\text{H}}$  2.68/ $\delta_{\text{C}}$  36.1 ppm assigned to C-6 and C-8, respectively, revealing its inclusion into the extended spin system of Ring B. To unambiguously determine the positions of acetyl and angeloyl moieties in **1**, HMBC spectrum was useful where it revealed clear long-range correlations from two methine protons at  $\delta_{\text{H}}$  4.79 (H-2) and  $\delta_{\text{H}}$  5.00 (H-6) ppm to two carboxyl carbons at  $\delta_{\text{C}}$  170.2 and  $\delta_{\text{C}}$  168.4 ppm assigned for C-1' and C-1'' from acetyl and angeloyl moieties, respectively. Based on the obtained results, compound **1** was identified as a new tricyclic sesquiterpene lactone congener with a rare eight-membered ring as ring B. Compound **1** was trivially named as photodactolide A.

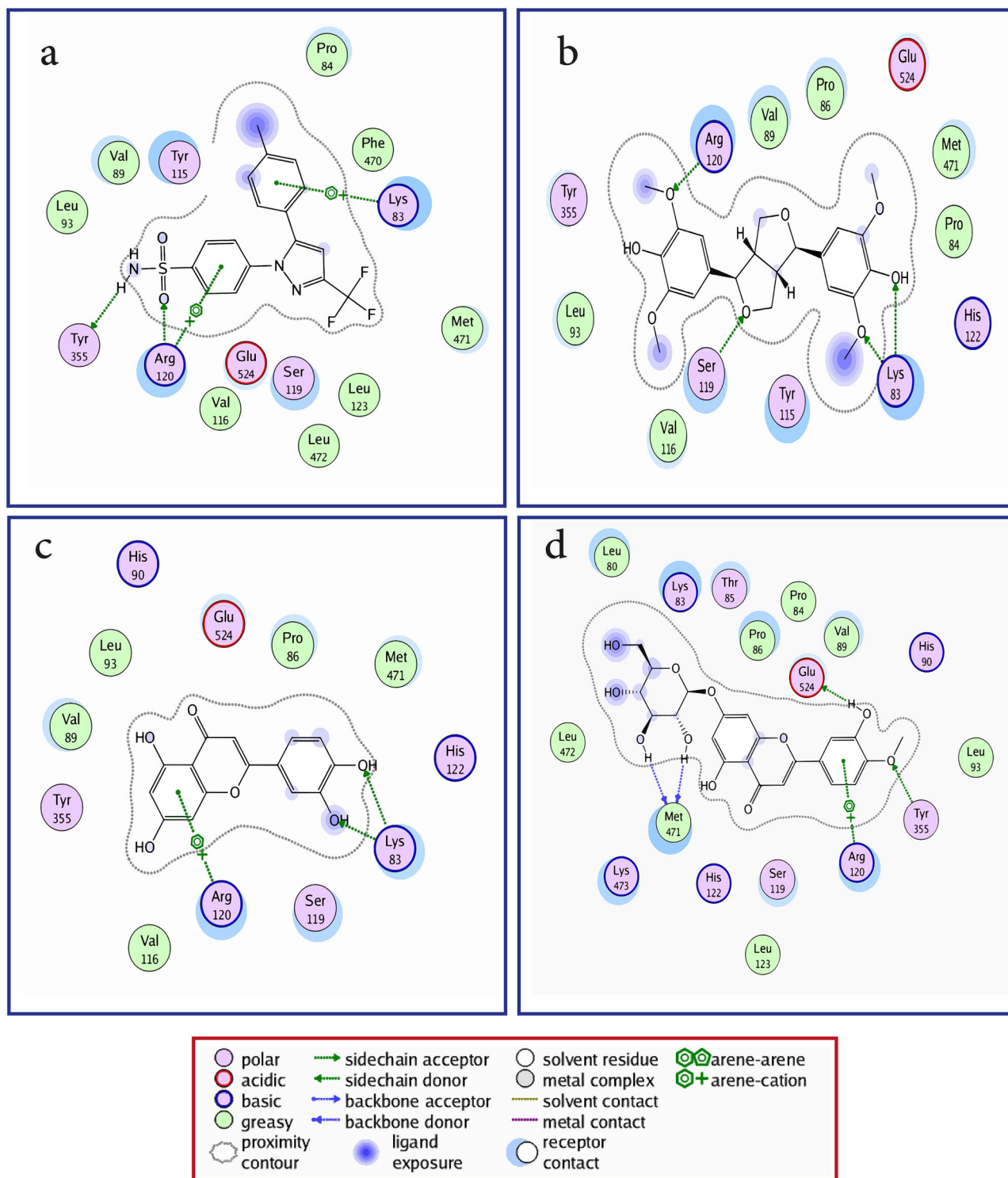


**Figure 3.** 2D binding mode and residues involved in the recognition of (a) celecoxib, the most potent compounds (b) **4**, (c) **7**, and (d) **8** docked and minimized in the COX-2 binding pocket.

The relative configuration of **1** was determined based on ROESY spectrum (Figure 2) that revealed clear correlations between H-2, H-6, H-9/CH<sub>3</sub>-16 indicating that H-2, H-6, H-9 and CH<sub>3</sub>-16 are all facing the same side of the molecule and featuring  $\beta$ -configuration. While the  $\alpha$ -configuration of the protons at C-1, C-8 and C-14 was proved by the ROESY correlations between H-1 and CH<sub>3</sub>-14/H-8. Attempts were carried out to determine the absolute configuration using electronic circular dichroism (ECD) measurements but were unsuccessful. The

reason was that after NMR measurements, the spectrum indicated decomposition of the compound either during storage or because of using deuterated chloroform for NMR analysis.

#### *In vitro* assay against *Helicobacter pylori*

All isolated compounds were evaluated for their antibacterial activity against *H. pylori* and the results are shown in (Table 2).

**Table 4.** The COX-2 enzyme inhibition (IC<sub>50</sub> μM), docking scores<sup>a</sup> and type of binding interactions of the tested isolated compounds and the reference compound (celecoxib).

| Compound                              | COX-2 inhibition (IC <sub>50</sub> μM) | Binding energy (Kcal/mol) (docking score) | Type of binding interactions  |
|---------------------------------------|--|---|---|
| Celecoxib                             | 0.28 ± 0.41                            | -14.7                                     | <ul style="list-style-type: none"> <li>• H-bonds with Arg120 and Tyr355</li> <li>• Arene-cation interaction with Arg120 and Lys83</li> <li>• Strong hydrophobic interaction with Tyr115, Ser119, Pro84 and Val89</li> </ul>                                 |
| Photodactolide A (1)                  | NA                                     | -11.1                                     | <ul style="list-style-type: none"> <li>• Hydrophobic interaction with Lys83 and Ser119</li> </ul>   |
| Pimaric acid (2)                      | 5.6 ± 0.14                             | -12.4                                     | <ul style="list-style-type: none"> <li>• H-bonds with Ser119</li> <li>• Strong hydrophobic interaction with Arg120 and Lys83</li> </ul>   |
| Vaginatin (3)                         | NA                                     | -11.0                                     | <ul style="list-style-type: none"> <li>• Hydrophobic interaction with Lys83 and Met471</li> </ul>   |
| Syringaresinol (4)                    | 1.04 ± 0.63                            | -17.7                                     | <ul style="list-style-type: none"> <li>• Two H-bonds with Lys83</li> <li>• H-bonds with Ser119 and Arg120</li> <li>• Strong hydrophobic interaction with Tyr115, Met471 and Val89</li> </ul>  |
| Chrysoeriol (5)                       | 6.6 ± 0.74                             | -7.9                                      | <ul style="list-style-type: none"> <li>• Strong hydrophobic interaction with Lys83 and Lys473</li> </ul>  |
| Apigenin (6)                          | 3.2 ± 1.4                              | -7.8                                      | <ul style="list-style-type: none"> <li>• Strong hydrophobic interaction with Met471, Lys83, Thr85 and Lys473</li> </ul>   |
| Luteolin (7)                          | 0.65 ± 0.33                            | -14.2                                     | <ul style="list-style-type: none"> <li>• Two H-bonds with Lys83</li> <li>• Arene-cation interaction with Arg120</li> <li>• Strong hydrophobic interaction with Ser119 and Val89</li> </ul>  |
| Diosmetin-7-O-β-D-glucopyranoside (8) | 0.45 ± 0.85                            | -15.5                                     | <ul style="list-style-type: none"> <li>• H-bonds with Tyr355 and Glu524</li> <li>• Two H-bonds with Met471</li> <li>• Arene-cation interaction with Arg120</li> <li>• Strong hydrophobic interaction with Lys83, Ser119, Pro86, Leu80 and Lys473</li> </ul> |
| Methylparaben (9)                     | 14.9 ± 0.63                            | -6.2                                      | <ul style="list-style-type: none"> <li>• Hydrophobic interaction with Ser119 and Arg120</li> </ul>  |
| p-Hydroxybenzoic acid (10)            | 2.7 ± 1.3                              | -8.5                                      | <ul style="list-style-type: none"> <li>• H-bonds with Ser119 and Glu524</li> <li>• Arene-cation interaction with Arg120</li> <li>• Strong hydrophobic interaction with Val89</li> </ul>   |
| Methyl β-D-xylopyranoside (11)        | 5.9 ± 1.2                              | -7.7                                      | <ul style="list-style-type: none"> <li>• Strong hydrophobic interaction with Lys83 and Ser119</li> </ul>  |

• Celecoxib was used as reference compound. • All data are presented as mean value ± SD for three independent experiments. • NA: no activity.

<sup>a</sup>Docking was performed following the reported procedure (Qandeel et al. 2020) towards the active site of cyclooxygenase-2 (COX-2) enzyme (PDB code ID: 5IKQ).

Several compounds revealed potential anti-*H. pylori* activities including **10** which showed a potent activity (MIC = 0.48 μg/mL). However, compounds **4**, **6**, **8** and **9** exhibited MICs ranging between 0.98 and 1.95 μg/mL that is equal or even more potent compared to the standard drug clarithromycin (MIC = 1.95 μg/mL). Amongst the other tested compounds, moderate to low inhibitory activities were noticed for **2**, **5**, **7** and **11** while **1** and **3** were not active against *H. pylori*.

### Evaluation of in vitro anti-inflammatory activity against cyclooxygenase-2 (COX-2) enzyme

The samples were tested in order to investigate the anti-inflammatory response by inhibiting COX-2 enzyme. The obtained results (Table 3) illustrated the anti-inflammatory activities of isolated compounds (**1–11**) compared to celecoxib as a reference drug (IC<sub>50</sub> value = 0.28 ± 0.41 μg/mL). Among the tested compounds, diosmetin-7-O-β-D-glucopyranoside (**8**) was the most active with an IC<sub>50</sub> value of 0.45 ± 0.85 μg/mL, followed by luteolin (**7**) (0.65 ± 0.33 μg/mL) then syringaresinol (**4**) (1.04 ± 0.63 μg/mL).

### Molecular docking simulation

Docking results of compounds (**1–11**) to COX-2 enzyme active site, using celecoxib as a standard drug, showed the types of binding interactions and binding scores of these compounds (Figure 3 and Table 4). Celecoxib (binding score = -14.7 kcal/mol) bound to COX-2 active site via two hydrogen bonds with Arg120 and Tyr355 by its sulfonamide moiety. In addition, it bound to COX-2 via two arene-cation interactions with Arg120

and Lys83 by its two-phenyl moieties and through strong hydrophobic interaction with Tyr115, Ser119, Pro84 and Val89.

Compounds **4**, **7** and **8** (IC<sub>50</sub> values of 1.04, 0.65 and 0.45 μM, respectively) showed the best docking results. Compounds **4**, **7** and **8** shared with celecoxib in common its binding with Arg120, Lys83 and Ser119 amino acid residues.

Both compounds **4** and **7** (binding score = -17.7 and -14.2 kcal/mol) bound to Lys83 via two hydrogen bonds; **4** by its ether and phenolic hydroxyl groups, while **7** by its catechol hydroxyl groups. They also bound with Arg120; **4** bound via hydrogen bond (H-bond) by its phenyl methoxy group, while **7** via arene-cation interaction by its 5,7-dihydroxy-4H-chromen-4-one aromatic system. Compound **4** also bound to Ser119 via hydrogen bond by tetrahydrofuran ring.

Compound **8** (binding score = -15.5 kcal/mol) bound to Tyr355, Glu524 and Met471 via four hydrogen bonds; two H-bonds with Met471 by its 7-O-glycoside and H-bond with Glu524 by its 3'-hydroxy substituent and the last one with Tyr355 by its 4'-methoxy substituent. Compound **8** also bound to Arg120 via arene-cation interaction by its 2-(3-hydroxy-4-methoxyphenyl) moiety.

The other predicted binding interactions of the tested compounds with COX-2 enzyme active site were tabulated in supplementary materials.

### Three-dimensional aligned conformations

The 3D binding pocket surface mapping showed that the most potent anti-inflammatory compounds **4**, **7** and **8** occupied and filled the whole space of binding pockets on COX-2 active site in a comparable way to that of celecoxib (Table 5).

**Table 5.** Three-dimension interactions and surface maps within the COX-2 binding pocket for the standard drug celecoxib and the most potent compounds 4, 7 and 8.

| Isolated comp.                        | 3D interactions | 3D surface map |
|---------------------------------------|-----------------|----------------|
| Celecoxib                             |                 |                |
| Syringaresinol (4)                    |                 |                |
| Luteolin (7)                          |                 |                |
| Diosmetin-7-O-β-D-glucopyranoside (8) |                 |                |

## Discussion

The petroleum ether fraction of *P. dactylifera* L. CV 'Zaghloul' fibrous mesh presented photodactolide A (**1**) as a new tricyclic sesquiterpene lactone derivative with a rare eight-membered ring. The structure was elucidated based on extensive 1D and 2D NMR spectra. To the best of our knowledge, it is the first report of compounds (**2–11**) from agricultural waste of date palm. Moreover, compounds (**2–4**, **8** and **11**) were isolated for the first time from the genus *Phoenix*.

The World Health Organization (WHO) has designated *Helicobacter pylori*, a virulent Gram-negative pathogen, as a Class I carcinogen for gastric cancer (Kouitchou Mabeku et al. 2017). Currently, the infection is widespread worldwide, with a higher prevalence in developing regions (Zhao et al. 2022). Since gastritis is the most common symptom of *H. pylori* infection, many studies have focused on how the gastric inflammatory response works and how to control the disease (Masadeh et al. 2014). In order to develop a natural, affordable, and effective medication, the current study evaluated the anti-*H. pylori* and anti-inflammatory potential against COX-2 enzyme of all isolated compounds. Intriguingly, in the *in vitro* assays, syringaresinol (**4**), luteolin (**7**) and diosmetin-7-O- $\beta$ -D-glucopyranoside (**8**) isolated from waste parts of *P. dactylifera* L. (CV 'Zaghloul') exhibited strong inhibitory activities against both *H. pylori* and cyclooxygenase (COX-2) enzyme. These results are consistent with those of earlier research reporting the anti-*H. pylori* activity of the lignan derivative syringaresinol (Miyazawa et al. 2006). In addition, flavonoid aglycones and glycosides such as luteolin and diosmetin-7-O- $\beta$ -D-glucopyranoside are well-known for their antioxidant, anti-inflammatory and anti-*H. pylori* properties (Radziejewska et al. 2020; Jafar et al. 2021; Garg et al. 2022). This article demonstrated how research on date palm agricultural waste produced valuable phytoconstituents with potential activities that can be taken as a cornerstone for further research to develop phytopharmaceuticals.

### Structure-activity relationship (SAR)

Isolated compounds (**1–11**) were investigated *in vitro* and *in silico* for their COX-2 enzyme inhibition. Molecular docking studies showed that compounds (**4**, **7** and **8**) have the best binding interactions with Arg120, Lys83 and Ser119, the key amino acid residues at COX-2 active site, by their bulky polar structure. Based on the obtained results, the following SARs could be concluded:

Among the polyphenolic derivatives, compounds, diosmetin-7-O- $\beta$ -D-glucopyranoside (**8**) showed the best COX-2 inhibition potency. This strong potency could be attributed to the 7-O-glucoside moiety that bound to the active site key amino acids *via* two hydrogen bonds and other strong hydrophobic interactions. These results may also indicate that the free 3'-hydroxy substituent is better than 3'-methoxy substituent and 3'-unsubstituted derivatives. These may be proved by comparing the docking scores of luteolin (**7**) with 3'-hydroxy substituent and diosmetin-7-O- $\beta$ -D-glucopyranoside (**8**) featuring also 3'-hydroxy substituent, the most potent COX-2 inhibitors, found to bind to the active site key amino acids *via* strong hydrogen bonding interactions compared to the low potency of chrysoeriol (**5**) that has 3'-methoxy or apigenin (**6**) that has no substituent at 3' position.

For lignan derivatives syringaresinol (**4**), the 4,4' tetrahydro-1H,3H-furo[3,4-c]furan fused ring system showed no significant advantage over that of 5,7-dihydroxy-2-phenyl-4H-chromen-4-

one in compounds (**5–8**). Generally, bulky polar derivatives showed better binding interactions with the COX-2 active site key amino acids and better COX-2 inhibition activity.

## Conclusion

This study displayed that date palm wastes could be exploited for the production of valuable phytoconstituents with variable anti-*H. pylori* activities. Eleven compounds were isolated from date palm wastes including one designated as a new natural product along with other terpenoidal metabolites, lignan and polyphenolic derivatives. All isolated compounds were evaluated for their antibacterial activity against *H. pylori* and anti-inflammatory activity against COX-2 enzyme. Compounds **4**, **8** and **10** showed promising activity against *H. pylori* compared to the reference drug. In addition, compounds **4**, **7** and **8** were very potent COX-2 enzyme inhibitors. *In silico* model supports that the most effective anti-inflammatory compounds (**4**, **7** and **8**) occupied and filled the entire space of binding pockets on COX-2 active site in a manner similar to that of celecoxib. Therefore, the present study features syringaresinol (**4**) and diosmetin-7-O- $\beta$ -D-glucopyranoside (**8**) as new and effective *H. pylori* and COX-2 inhibitors that could be candidates for future *in vivo* research projects aiming at lead development for new peptic ulcer therapeutics.

NMR and MS spectra of all isolated compounds (**1–11**), as well as growth inhibition curves and 2D molecular docking pictures are available online.

## Acknowledgements

The authors would like to acknowledge assistant lecturer Mohamed A. Sabry for helping in molecular docking study.

## Disclosure statement

No potential conflict of interest was reported by the author(s).

## Funding

The author(s) reported there is no funding associated with the work featured in this article.

## References

- Abou Baker D. 2020. Plants against *Helicobacter pylori* to combat resistance: an ethnopharmacological review. *Biotechnol Rep.* 26:e00470.
- Alwahsh MAA, Khairuddean M, Chong WK. 2015. Chemical constituents and antioxidant activity of *Teucrium barbeyanum* Aschers. *Rec Nat Prod.* 9(1):159–163.
- Amessis-Ouchemoukh N, Madani K, Falé PLV, Serralheiro ML, Araújo MEM. 2014. Antioxidant capacity and phenolic contents of some Mediterranean medicinal plants and their potential role in the inhibition of cyclooxygenase-1 and acetylcholinesterase activities. *Ind Crops Prod.* 53:6–15.
- Aydeniz-Güneşer B. 2022. Valorization of date palm (*Phoenix dactylifera*) wastes and by-products. In: Ramadan MF, Farag MA, editors. *Mediterranean fruits bio-wastes*. Cham: Springer; p. 391–402.
- Baliga MS, Baliga BRV, Kandathil SM, Bhat HP, Vayalil PK. 2011. A review of the chemistry and pharmacology of the date fruits (*Phoenix dactylifera* L.). *Food Res Int.* 44(7):1812–1822.
- Bashyal P, Parajuli P, Pandey RP, Sohng JKJC. 2019. Microbial biosynthesis of antibacterial chrysoeriol in recombinant *Escherichia coli* and bioactivity assessment. *Catalysts.* 9(2):112.

- Bentrad N, Hamida-Ferhat A. 2020. Date palm fruit (*Phoenix dactylifera*): nutritional values and potential benefits on health. In: Preedy VR, Watson RR, editors. The Mediterranean diet. Amsterdam: Elsevier; p. 239–255.
- Bonacorsi C, Raddi MSG, Carlos IZ, Sannomiya M, Vilegas WJBC, Medicine A. 2009. Anti-*Helicobacter pylori* activity and immunostimulatory effect of extracts from *Byrsonima crassa* Nied.(Malpighiaceae). BMC Complementary Altern Med. 9(1):1–7.
- Dang NH, Zhang X, Zheng M, Son KH, Chang HW, Kim HP, Bae K, Kang SS. 2005. Inhibitory constituents against cyclooxygenases from *Aralia cordata* Thunb. Arch Pharm Res. 28(1):28–33.
- El-Far AH, Oyinloye BE, Sepehrimanesh M, Allah MAG, Abu-Reidah I, Shaheen HM, Razeghian-Jahromi I, Alsenosy AEA, Noreldin AE, Al Jaouni SK, et al. 2019. Date palm (*Phoenix dactylifera*): novel findings and future directions for food and drug discovery. Curr Drug Discov Technol. 16(1):2–10.
- Faiad A, Alsmari M, Ahmed MMZ, Bouazizi ML, Alzahrani B, Alrobei H. 2022. Date palm tree waste recycling: treatment and processing for potential engineering applications. Sustainability. 14(3):1134.
- Galal AM, Mohamed HS, Abdel-Aziz MM, Hanna AG. 2021. Development, synthesis, and biological evaluation of sulfonyl- $\alpha$ -L-amino acids as potential anti-*Helicobacter pylori* and IMPDH inhibitors. Arch Pharm. 354(6): e2000385.
- Garg M, Chaudhary SK, Goyal A, Sarup P, Kumari S, Garg N, Vaid L, Shiveena B. 2022. Comprehensive review on therapeutic and phytochemical exploration of diosmetin: a promising moiety. Phytomedicine Plus. 2(1):100179.
- Jafar M, Salahuddin M, Khan MSA, Alshehry Y, Alrwaili NR, Alzahrani YA, Imam SS, Alshehri S. 2021. Preparation and *in vitro-in vivo* evaluation of luteolin loaded gastroretentive microsphere for the eradication of *Helicobacter pylori* infections. Pharmaceutics. 13(12):2094.
- Jonoobi M, Shafie M, Shirmohammadi Y, Ashori A, Hosseinabadi HZ, Mekonnen T. 2019. A review on date palm tree: properties, characterization and its potential applications. J Renewable Mater. 7(11):1055–1075.
- Kouitcheu Mabeku LB, Eyoun Bille B, Tchouangueu TF, Nguépi E, Leundji H. 2017. Treatment of *Helicobacter pylori* infected mice with *Bryophyllum pinnatum*, a medicinal plant with antioxidant and antimicrobial properties, reduces bacterial load. Pharm Biol. 55(1):603–610.
- Lee SY, Kim KH, Lee IK, Lee KH, Choi SU, Lee KR. 2012. A new flavonol glycoside from *Hylomecon vernalis*. Arch Pharm Res. 35(3):415–421.
- Malee T. 2011. Chemical constituents from the leaves and stems of *Citrus aurantifolia* swingle [master's thesis]. Bangkok: Prince of Songkla University.
- Masadeh MM, Alkofahi AS, Alzoubi KH, Tumah HN, Bani-Hani K. 2014. Anti-*Helicobacter pylori* activity of some Jordanian medicinal plants. Pharm Biol. 52(5):566–569.
- McEwan T, McInnes AG, Smith DG. 1982.  $^1\text{H}$ - and  $^{13}\text{C}$ -NMR spectra of the methyl mono-, di-, and tri-*O*-acetyl- $\alpha$ - and - $\beta$ -D-xylopyranosides. Carbohydrate Res. 104(2):161–168.
- Miyazawa M, Utsunomiya H, Inada K-i, Yamada T, Okuno Y, Tanaka H, Tatematsu M. 2006. Inhibition of *Helicobacter pylori* motility by (+)-syringaresinol from unripe Japanese apricot. Biol Pharm Bull. 29(1): 172–173.
- Orlando BJ, Malkowski MG. 2016. Substrate-selective inhibition of cyclooxygenase-2 by fenamic acid derivatives is dependent on peroxide tone. J Biol Chem. 291(29):15069–15081.
- Park S, Yang S, Ahn D, Yang JH, Kim DK. 2011. Antioxidative phenolic compounds from the whole plant of *Juncus diastrophanthus*. J Korean Soc Appl Biol Chem. 54(5):685–692.
- Petrovic N, Murray M. 2010. Using *N, N, N', N'*-tetramethyl-*p*-phenylenediamine (TMPD) to assay cyclooxygenase activity *in vitro*. In: Armstrong D, editor. Advanced protocols in oxidative stress II. Cham: Springer; p. 129–140.
- Qandeel NA, El-Damasy AK, Sharawy MH, Bayomi SM, El-Gohary NS. 2020. Synthesis, *in vivo* anti-inflammatory, COX-1/COX-2 and 5-LOX inhibitory activities of new 2, 3, 4-trisubstituted thiophene derivatives. Bioorg Chem. 102:103890.
- Radziejewska I, Borzym-Kluczyk M, Leszczyńska K. 2020. Luteolin alters MUC1 extracellular domain, sT antigen, ADAM-17, IL-8, IL-10 and NF- $\kappa$ B expression in *Helicobacter pylori*-infected gastric cancer CRL-1739 cells: a preliminary study. Biomed Rep. 14(2):1–1.
- Rao P, Rathod V. 2019. Valorization of food and agricultural waste: a step towards greener future. Chem Rec. 19(9):1858–1871.
- Roy A, Milonuzzaman M, bin Kader F, Islam A, Alam MK, Hasan J, Faisal MS, Asaduzzaman SM, Rahman M, Majumder M. 2019. *In silico* molecular docking of some isolated selected compounds of *Phoenix sylvestris* (L.) for analgesic activity. Biomed J Sci Tech Res. 16:11887–11891.
- Rustaiyan A, Sigari H, Jakupovic J, Grenz M. 1989. A sesquiterpene lactone from *Artemisia diffusa*. Phytochemistry. 28(10):2723–2725.
- Suleiman RK, Iali W, El Ali B, Umoren SA. 2021. New constituents from the leaves of date palm (*Phoenix dactylifera* L.) of Saudi origin. Molecules. 26(14):4192.
- Tian S, Chai X, Zan K, Zeng K, Guo X, Jiang Y, Tu P. 2013. Arvestolidides A–C, new rare sesquiterpenes from the aerial parts of *Artemisia vestita*. Tetrahedron Lett. 54(37):5035–5038.
- Wang Y-C. 2014. Medicinal plant activity on *Helicobacter pylori* related diseases. World J Gastroenterol. 20(30):10368–10382.
- Wong BCY, Zhang L, Ma J-L, Pan K-F, Li J-Y, Shen L, Liu W-D, Feng G-S, Zhang X-D, Li J, et al. 2012. Effects of selective COX-2 inhibitor and *Helicobacter pylori* eradication on precancerous gastric lesions. Gut. 61(6): 812–818.
- Wu P, Li X-G, Liang N, Wang G-C, Ye W-C, Zhou G-X, Li Y-L. 2012. Two new sesquiterpene lactones from the supercritical fluid extract of *Centipeda minima*. J Asian Nat Prod Res. 14(6):515–520.
- Wu P, Su M-X, Wang Y, Wang G-C, Ye W-C, Chung H-Y, Li J, Jiang R-W, Li Y-L. 2012. Supercritical fluid extraction assisted isolation of sesquiterpene lactones with antiproliferative effects from *Centipeda minima*. Phytochemistry. 76:133–140.
- Xue P-H, Zhang N, Liu D, Zhang Q-R, Duan J-S, Yu Y-Q, Li J-Y, Cao S-J, Zhao F, Kang N, et al. 2021. Cytotoxic and anti-inflammatory sesquiterpenes from the whole plants of *Centipeda minima*. J Nat Prod. 84(2): 247–258.
- Yang R-L, Yan Z-H, Lu Y. 2008. Cytotoxic phenylpropanoids from carrot. J Agric Food Chem. 56(9):3024–3027.
- Yoshioka T, Inokuchi T, Fujioka S, Kimura Y. 2004. Phenolic compounds and flavonoids as plant growth regulators from fruit and leaf of *Vitex rotundifolia*. Z Naturforsch C J Biosci. 59(7-8):509–514.
- Zhang X, He J, Huang W, Huang H, Zhang Z, Wang J, Yang L, Wang G, Wang Y, Li Y. 2018. Antiviral activity of the sesquiterpene lactones from *Centipeda minima* against influenza A virus *in vitro*. Nat Prod Commun. 13:115–119.
- Zhao S, Wan D, Zhong Y, Xu X. 2022.  $1\alpha, 25$ -Dihydroxyvitamin D3 protects gastric mucosa epithelial cells against *Helicobacter pylori*-infected apoptosis through a vitamin D receptor-dependent c-Raf/MEK/ERK pathway. Pharm Biol. 60(1):801–809.